Higher Order Effects in the Dielectric Constant of Percolative Metal-Insulator Systems above the Critical Point

W.D. Heiss, D.S. McLachlan and C. Chiteme

Department of Physics

University of the Witwatersrand, PO Wits 2050, Johannesburg, South Africa

The dielectric constant of a conductor–insulator mixture shows a pronounced maximum above the critical volume concentration. Further experimental evidence is presented as well as a theoretical consideration based on a phenomenological equation. Explicit expressions are given for the position of the maximum in terms of scaling parameters and the (complex) conductances of the conductor and insulator. In order to fit some of the data, a volume fraction dependent expression for the conductivity of the more highly conductive component is introduced.

The ac and dc conductivities of resistor and resistor-capacitor (RC) networks and continuum conductor-insulator composites have been extensively studied for many years. In systems where there is a very sharp change (metal-insulator transition or MIT) in the dc conductivity at a critical volume fraction or percolation threshold denoted by ϕ_c, the most successful models, for both the dc and ac properties, have proved to be approaches using percolation theory. Early work concentrated on the dc properties, but since it was realized that the percolation threshold is a critical point, and that the percolation equations could be arrived at from a scaling relation, several papers ([1] and the references therein), reporting experimental results on the ac conductivity have appeared. Review articles, containing the theory and some experimental results, on the complex ac conductivity and other properties of binary metal-insulator systems include [2]- [4].

In [1], [5] and [6] the following equation was introduced

$$\frac{(1-\phi)(\sigma_I^{1/s} - \sigma_M^{1/s})}{(\sigma_I^{1/s} + A\sigma_M^{1/s})} + \frac{\phi(\sigma_C^{1/t} - \sigma_M^{1/t})}{(\sigma_C^{1/t} + A\sigma_M^{1/t})} = 0, \qquad (1)$$

which gives a phenomenological relationship between σ_C, σ_I, and σ_M. They are, respectively, the conductivities of the conducting and insulating component and the mixture of the two components. Note that all three quantities σ_C, σ_I, and σ_M can be real or complex numbers in Eq.(1). The conducting volume fraction ϕ ranges between 0 and 1 with $\phi = 0$ characterizing the pure insulator substance ($\sigma_M \equiv \sigma_I$) and $\phi = 1$ the pure conductor substance ($\sigma_M \equiv \sigma_C$). The critical volume fraction, or percolation threshold is denoted by ϕ_c, where a transition from an essentially insulating to an essentially conducting medium takes place, and $A = (1 - \phi_c)/\phi_c$. For $s = t = 1$ the equation is equivalent to the Bruggeman

symmetric media equation [7]. Equation (1) yields the two limits

$$|\sigma_C| \to \infty: \qquad \sigma_M = \sigma_I \frac{\phi_c^s}{(\phi_c - \phi)^s} \qquad \phi < \phi_c \quad (2)$$

$$|\sigma_I| \to 0: \qquad \sigma_M = \sigma_C \frac{(\phi - \phi_c)^t}{(1 - \phi_c)^t} \qquad \phi > \phi_c \quad (3)$$

which characterize the exponents s and t. Note that Eqs. (2) and (3) are the normalized percolation equations. At $\phi = \phi_c$,

$$\sigma_{MC} = \sigma_C / A^{(st)/(s+t)} \left(\sigma_I/\sigma_C\right)^{t/(s+t)} \quad (4)$$

up to higher order terms in σ_I/σ_C.

Thus, in the crossover region where ϕ lies between $\phi_c - (\sigma_I/\sigma_C)^{1/(s+t)}$ and $\phi_c + (\sigma_I/\sigma_C)^{1/(s+t)}$ we have [2]- [4]

$$\sigma_M \propto \sigma_I^{t/(s+t)} \sigma_C^{s/(s+t)}. \quad (5)$$

When using the above equation to analyze ac systems the complex conductivities ($\sigma_x = \sigma_{xr} - i\omega\epsilon_o\epsilon_{rx}$, where ω is the angular frequency, ϵ_o the permittivity of free space and ϵ_{rx} the real relative dielectric constant of the component) must be inserted in Eq.(1). Below ϕ_c the leading term yields the imaginary conductivity or real dielectric constant, while the next order term gives the real conductivity. In turn, above ϕ_c the real conductivity is the leading term and the real dielectric constant appears in the next order term, upon which the present paper focuses. In many instances the approximation $\sigma_C = \sigma_{cr}$ and $\sigma_I = -i\omega\epsilon_o\epsilon_r$ is made [2]- [4]. In this case, the crossover region ranges over ϕ between $\phi_c - (\omega\epsilon_o\epsilon_r/\sigma_C)$ and $\phi_c + (\omega\epsilon_o\epsilon_r/\sigma_C)$. This means that, as a function of frequency, a sample with ϕ close to ϕ_c will enter an experimentally observable crossover region for sufficiently large ω and eventually obey Eq. (5) with a frequency dependence of $\omega^{t/(s+t)}$ for both the real and imaginary parts.

In a series of papers reporting on the dc [5] and ac [1,6] conductivities of three Graphite-Boron Nitride system systems it was shown theoretically that

1. the scaling relations derived from the first order terms of Eq.(1), above and below ϕ_c, had the frequency dependencies required by the classical scaling ansatz [2]- [4] (dc scaling is dealt with in [8]);

2. the second order scaling relations, derived from Eq.(1), in the crossover region, had the frequency and $(\phi - \phi_c)$ dependencies required by the classical scaling ansatz [2]- [4];

3. the second order scaling relations, in the region where the first order terms obey Eqs.(2) and (3), were not in agreement with the classical scaling ansatz [6];

4. the loss or conductivity term in the dielectric state had a frequency exponent of $(1 + t)/t$ and not 2 as required by the classical ansatz [2]- [4].

Experimentally it was shown that

1. the first order experimental results for the G-BN systems could be scaled onto separate curves above and below ϕ_c and that these scaled curves could be fitted by the scaling functions generated by Eq.(1), for all ϕ and ω values [5]. This was also found to be the case by Chiteme and McLachlan [9] for "cellular" percolation systems, some of the dc properties of which are given in [10];

2. after taking the loss (conductivity) term of the dielectric component into account the exponent for the loss was much closer to $(1+t)/t$ than to 2 [6];

3. the real dielectric constant, when plotted as a function of ϕ for the fixed ω, does not peak at ϕ_c but continues to increase reaching a peak at a value of ϕ greater than ϕ_c. The resultant curve has a hump like appearance and the position of the peak depends on ω, ϵ_{ir} and σ_C. It was then shown [6] that this behavior could be qualitatively modeled by Eq.(1).

In the present paper progress is reported on this last point. We begin with a further theoretical investigation of the behavior of the dielectric constant ϵ just above ϕ_c. Since σ_M is in general the result of finding numerically the root of a transcendental equation, this can only be achieved by expanding σ_M around ϕ_c. With the ansatz $\sigma_M(\phi)^{1/t} = \sigma_{MC}^{1/t} + \delta$ we obtain from Eq.(1)

$$\delta = \frac{\sigma_{MC}^{1/t}\sigma_I^{1/s}(A-1) + \Delta\phi\,\sigma_C^{1/t}\sigma_{MC}^{1/s}}{A(t/s+1)\sigma_{MC}^{1/s} - t/s\,\Delta\phi\,\sigma_C^{1/t}\sigma_{MC}^{1/s-1/t} - (A-1)\sigma_I^{1/s}} \quad (6)$$

with $\Delta\phi = (\phi-\phi_c)/\phi_c$. Note that δ does not vanish when $\Delta\phi = 0$ as we have to take into account additional terms of lower order which do not vanish for $\phi = \phi_c$. These terms are omitted in Eq.(4) but they are of the same order as terms linear in $\phi - \phi_c$ and must be incorporated for reasons of consistency. Inserting the right hand side of Eq.(4) for σ_{MC} it is now straightforward, albeit tedious, to obtain the position of the maximum of the imaginary part. The calculation yields for the maximum

$$\phi_{\max} = \phi_c + \frac{s+t}{2t}\frac{(1-\phi_c)(1-2\phi_c)}{\phi_c}A^{-\frac{2s}{s+t}}\left(\frac{|\sigma_I|}{\sigma_C}\right)^{\frac{2}{s+t}} \quad (7)$$
$$+ \mathcal{O}\left(\left(\frac{\sigma_I}{\sigma_C}\right)^{\frac{3}{s+t}}\right).$$

We emphasize that the deviation of $\phi_{\max}$ from ϕ_c is obtained only when the expansion in powers of $(\sigma_I/\sigma_C)^{1/(s+t)}$ is taken beyond the first power; in fact, the result given can be obtained only if the expressions are expanded up to the third power.
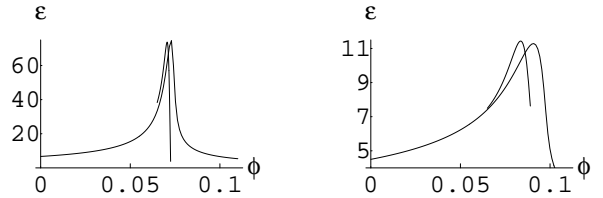

FIG. 1. Comparison of the analytic expression $\sigma_M(\phi)$ with the numerical solution for 10 Hz (left) and 1 Mhz (right). The curve for the analytic $\sigma_M(\phi)$ has been drawn only for values of ϕ where the analytic expression for $\delta(\phi)$ is supposed to be reliable. The parameters used are given in the text.

We have checked the reliability of this analytic expression by comparing with numerical solutions over a wide range of frequencies and are satisfied with its performance (see Figs.1). The parameters chosen in the illustration adhere to the Niobium Carbide system [6] which exhibits pronounced maxima beyond $\phi_c = 0.065$; they are $t = 5.46(4.71)$, $s = 0.75(0.40)$, $\sigma_C = 1.07 \cdot 10^4 (\Omega m)^{-1}$ and $\sigma_I = -i\omega\epsilon_0\epsilon_r$ with $\epsilon_r = 5.4(6.7)$ for the left (right) case. The difference between the two curves, even at $\phi = \phi_c$, reflects the error made by considering linear terms in δ only. Nevertheless, the analytic expression allows important conclusions to be drawn for the position of the maximum. Note that $\phi_{\max}$ does not depend on individual values of σ_I or σ_C, in other words the maximum position depends only on the ratio σ_I/σ_C (or equivalently on $\omega\epsilon_0\epsilon_r/\sigma_C$). Note in particular that

1. the deviation of $\phi_{\max}$ from ϕ_c starts with the second order term in $(\sigma_I/\sigma_C)^{1/(s+t)}$; recall that this first order term determines the width of the cross over region [2]- [4];

2. the larger the ratio σ_I/σ_C the further is the maximum pushed away from the transition point ϕ_c. In turn, the position of the maximum tends towards ϕ_c for $\sigma_I/\sigma_C \to 0$ as it should;

3. for finite values of the ratio σ_I/σ_C the distance $\phi_{\max} - \phi_c$ increases the more rapidly the more pronounced the inequality $s + t > 2$;

4. to lowest order, the frequency dependence of of the distance $\phi_{\max} - \phi_c$ is given by $\omega^{\frac{2}{s+t}}$.

2

The derivative of $\Im\sigma_M$ at ϕ_c is easier to obtain, but the result is slightly more involved. We here report the essential result

$$\frac{\mathrm{d}\Im\sigma_M}{\mathrm{d}\phi}|_{\phi_c} \propto \Im\left[\left(\frac{\sigma_I^{\frac{t}{s}}}{\sigma_C^{\frac{s}{t}}}\right)^{\frac{1}{s+t}}\sigma_I^{\frac{1}{s}}\sigma_C^{\frac{1}{t}}\right].$$

We stress that the derivatives of $\Re\sigma_M$ and $\Im\sigma_M$ at ϕ_c are always continuous and tend to zero for $(\sigma_I/\sigma_C) \to 0$.
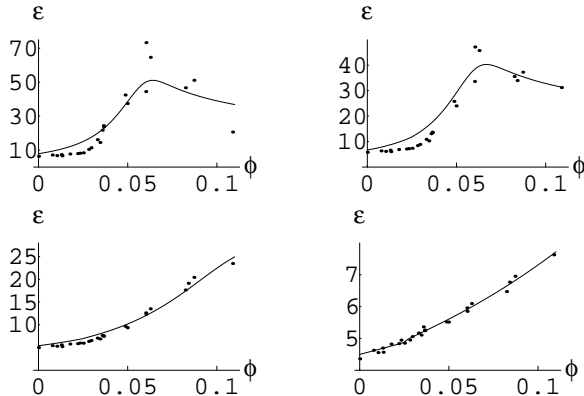

FIG. 2. Fits of experimental data at 1 Hz, 10 Hz, 1 KHz and 1 MHz (top left to bottom right) for conducting Fe_3O_4 grains in a wax coated talcum powder matrix. The parameters used are given in the text.

As it has now been established and confirmed experimentally in the present paper and in [6], Eq.(1) gives rise to the hump in the dielectric constant just above ϕ_c. However, as can be seen in [6], Eq.(1), as it stands, only qualitatively models the experimental data. In order to better fit the dielectric data we propose an effective dependence of σ_C on ϕ that is based in spirit on a model due to Balberg [11] for non–universal values of t. The model accounts for values of t higher than those allowed by the Random Void (RV) and Inverse Random Void model (IRV) [12,13]. In this model Balberg assumes that the resistance distribution function $h(\epsilon)$, where ϵ is the proximity parameter, has the form ϵ^{-w} as $\epsilon \to 0$ and does not tend towards a constant as in the RV and IRV models. Using the approach of [13,14] and keeping the underlying node links and blobs model [15], Balberg derives an expression for a non-universal t which is equal to the one obtained from the RV model when $w = 0$ but can give a larger t for $w > 0$. For $w > 0$ the model also shows that the average resistance in the network can diverge when $\phi \to \phi_c$. The increase in t beyond its universal value t_{un} as found by Balberg can be lumped into $t = t_{\mathrm{un}} + t_{\mathrm{nun}} + r$ where r is the extra contribution due to the *characteristic* resistance of the network diverging at $\phi \to \phi_c$. This increase in *characteristic* resistance is incorporated into Eq.(1) and hence also into Eqs.(2) and (3), by substituting σ_C with

$$\sigma_C^{\mathrm{eff}} = \sigma_{00} + \sigma_{c0}\left(\frac{\phi - \phi_c}{1 - \phi_c}\right)^r, \qquad \phi > \phi_c \qquad (8)$$

with $r > 0$. The solution of Eq.(1) should yield a continuous σ_M across ϕ_c, which means that the conductivity σ_C should nowhere vanish. As a consequence, σ_C must reach a non–zero value denoted by σ_{00} at ϕ_c which is expected to be considerably lower than σ_{c0}. To avoid too many parameters the simplest assumption was made for $\phi < \phi_c$, that is $\sigma_C \equiv \sigma_{00}$ This should be reasonably valid just below ϕ_c where our interest is focussed. We stress that the effect of the modification by Eq.(8) is virtually indiscernible with regard to first order effects for the solution σ_M of Eq.(1) or the corresponding percolation power laws (Eqs. (2) and (3)) in the region where the power laws are obeyed. Computer simulations show that using Eq.(8) or a constant σ_C in Eq.(1) causes a difference in $\sigma_M(\phi - \phi_c)$ $(\phi > \phi_c)$ or $\epsilon_M(\phi_c - \phi)$ $(\phi_c > \phi)$ which is too minute to be resolved from available experimental data. The same holds for dispersion plots against ω of σ_M above ϕ_c and ϵ_M below ϕ_c as given in [1]. For this reason it has never been necessary previously to consider the modification given by Eq.(8). However, in our context the higher order effects are discernible in the dielectric constant just beyond ϕ_c and can be fitted much more satisfactorily than in [6] using Eqs.(1) and (8).
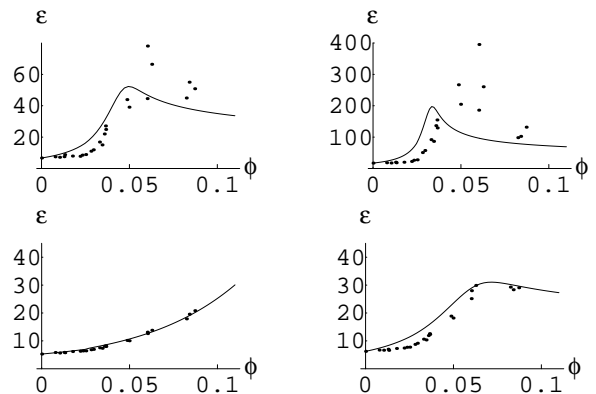

FIG. 3. Fits of experimental data at 1 Hz for $T = 25^0$ (top left) and $T = 120^0$ (top right). The bottom row displays corresponding results for 1 KHz. The system is the same as in Fig.2. The parameter values are given in the text.

In Fig.2 we display data and corresponding fits for conducting Fe_3O_4 grains in a wax coated talcum powder matrix [9,10]. The fits are far superior than those presented in [6]. We have chosen (somewhat arbitrarily) $\sigma_{00} = \sigma_C/10$ with the values $\sigma_C = \sigma_{c0} = 2.63 \cdot 10^{-1}(\Omega m)^{-1}$ obtained from extrapolating dc experimental results to $\phi = 1$, and $\sigma_I = -i\omega\epsilon_0\epsilon_r$ where ϵ_r is measured separately at each frequency. Good fits are obtained for $(t - r, r, s) = (4.7, 0.5, 0.97), (4.3, 0.7, 0.98), (4.4, 0.6, 1.0)$ and $(5.6, 0.4, 1.6)$ when moving from the top left to the bottom right display in Fig.2. The value $\phi_c = 0.025$, obtained from dc measurements, is used in Figs.2 and 3. Note that $t = t_{\mathrm{un}} + t_{\mathrm{nun}} + r$ is somewhat larger than the separately measured non-universal dc value of 4.2. Also note that in all cases it turned out that $r < 1$. This implies a steep increase of σ_C^{eff} just above ϕ_c. The fits

are not necessarily optimal as the multi-parameter landscape of the least square expression $|\sigma_M^{\exp} - \sigma_M^{\num}|^2$ in the parameters t, s and r (for fixed σ_{00}) has many local minima. However, the quality of the fits at the different local minima does not vary greatly for acceptable fits.

While this second order behavior of ϵ is in principle a complicated function of the various parameters the position of the maximum at $\phi_{\max}$ is essentially dependent only on the quotient σ_I/σ_C. This implies that a decrease of frequency (which is a decrease of σ_I) has an effect similar to a corresponding increase of σ_C, which can be obtained by an increase of temperature. This is convincingly demonstrated in Fig.3 where fits are obtained for the same system as in Fig.2 at different temperatures, i.e. at different values of σ_C and ϵ_r. The experimental data and the theoretical curves show that an increase in σ_C is equivalent to a decrease in ω (or σ_I). The experimental data appear somewhat erratic as they usually do for the low frequency chosen (1 Hz). The data in the first column of Fig.3 are slightly different from those in the first column of Fig.2 as the former are taken in a temperature controlled oven. Much better fits are obtained for higher frequencies as illustrated in the bottom row of Fig.3 (1 KHz) as the dielectric data are more reliable at higher frequencies. Similar to Fig.2, experimental values are used for $\epsilon_r(\omega, T)$ with $\sigma_{c0} = \sigma_C = 3.22 \cdot 10^{-1}(\Omega m)^{-1}$ at 25^0C and $\sigma_{c0} = \sigma_C = 1.42(\Omega m)^{-1}$ at 120^0C. The fits were obtained with the parameters $(t - r, r, s) = (4.65, 0.5, 1.0), (3.4, 0.6, 1.0), (4.4, 0.6, 1.0), (3.5, 0.9, 1.0)$ again choosing the fixed value $\sigma_{00} = \sigma_C/10$.
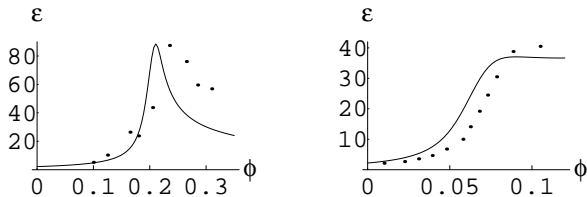

FIG. 4.   Fits of experimental data at 100 KHz of a water–oil emulsion using a hydrophil agent for uniform droplet size.

In continuum systems, all models for a non universal t are based on the premise [11]- [13] that a distribution of conductances exists in the conducting component which has a power law singularity. In a system where no such singularity occurs it should be possible to fit the data using Eq.(1), with t values closer to 2 and without the use of Eq.(8). A system *par excellence* which satisfies this requirement is a water-oil emulsion, using a surfactant to ensure uniform drop size. Data for such systems has been published in [16] -[18] and we present in Fig.4 data from Fig.1 of [16] and from Fig.4 of [17], which have been fitted using Eq.(1) with the same value of σ_C above and below ϕ_c. The values used, i.e. $\sigma_C = 1.9(1.5)(\Omega m)^{-1}$, $\sigma_I = -i\, 2 \cdot 10^{-11}\omega$, $\phi_c = 0.2(0.06)$ for the left (right) display and $\nu = 10^5$Hz are based on the dielectric and conductivity curves given in the

quoted papers. The fitting curves use $s = 1.15(1.35)$ and $t = 1.85(2.1)$. Note that the values of t are close to the universal value. Although better fits should be obtained with a more precise knowledge of the system parameters, these results show that using Eq.(8) as input in Eq.(1) is necessary to fit the dielectric data only when abnormally high values of t are observed in the dc data. Note that these data have been previously analyzed using Eq.(1) with a single exponent $(s = t)$ in [19].

To summarize: the pronounced hump observed experimentally for the dielectric constant of percolative metal insulator systems just above the critical concentration can be modeled using the higher order terms of Eq.(1) near ϕ_c. In the cases where t is well above the universal value Eq.(8) must be used to quantitatively model the dielectric data. Note also that all previous experiments on the dielectric constant "below" ϕ_c, where ϕ_c has not been independently measured by dc conductivity measurements, have probably incorrectly identified values of ϕ_c.

[1] Junjie Wu and D S McLachlan, Phys. Rev. B**58**, 14880 (1998).
[2] J P Clerc, G Girand, J M Langier and J M Luck, Adv. Phys. **39**, 191 (1990).
[3] D J Bergman and D Stroud, Solid State Physics **46**, edited by H Ehrenreich and D Turnbull (Academic Press, San Diego, 1992), p147.
[4] Ce-Wen Nan, Prog. Mater. Sci. **37**, 1 (1993).
[5] J Wu and D S McLachlan, Phys. Rev. B**56**, 1236 (1997).
[6] D S McLachlan, W D Heiss, C Chiteme and Junjie Wu, Phys. Rev. B**58** ,13558 (1998).
[7] D S McLachlan, M Blaskiewics and R Newnham, J. Am. Ceram. Soc. **73** , 2187 (1990).
[8] D S McLachlan, Physica B**254**, 249 (1998).
[9] C Chiteme and D S McLachlan, Physica A. to be published.
[10] C Chiteme and D S McLachlan, in *Electrically Based Microstructure Characterization*, MRS Proceedings 500, edited by R A Gerhardt, M A Alim and S R Taylor (Materials Research Society, Pittsburgh, 1998), p357.
[11] I Balberg, Phys. Rev. B**57**, 13351 (1998).
[12] B I Halperin, S Feng and P N Sen, Phys. Rev. Lett.**54**, 2391 (1985).
[13] S Feng, B.I. Halperin and P N Sen, Phys.Rev. B**35**, 1197 (1987).
[14] A-M S Tremblay, S Feng and P Breton, Phys. Rev. B**33**, R2077 (1986).
[15] D Stauffer and A Aharony *Introduction to Percolation Theory*, Taylor and Francis, London 1994.
[16] M A van Dijk, Phys. Rev. Letts. 55, 1003 (1985).
[17] M A van Dijk, G Castleliejn, J G H Joosten and Y K Levine, J Chem. Phys. **85**, 626 (1986).
[18] H F Eicke, S Geiger, F A Sauer and H Thomas, Ber.

Besenges. Phys. Chem. **90**, 872 (1986).

[19] D S McLachlan, Solid State Comm. **69**, 925 (1989).